ACS APPLIED MATERIALS & INTERFACES

Research Article

www.acsami.org

Bromo-Substituted Diketopyrrolopyrrole Derivative with Specific Targeting and High Efficiency for Photodynamic Therapy

Yu Cai,[†] Qianyun Tang,[†] Xiujuan Wu,[‡] Weili Si,[†] Qi Zhang,*[,‡] Wei Huang,*[,†] and Xiaochen Dong*[,†]

[†]Key Laboratory of Flexible Electronics (KLOFE) and Institute of Advanced Materials (IAM), Jiangsu National Synergetic Innovation Center for Advanced Materials (SICAM), and [‡]School of Pharmaceutical Sciences, Nanjing Tech University (NanjingTech), 30 South Puzhu Road, Nanjing 211816, China

Supporting Information

ABSTRACT: Novel photosensitizers with high reactive oxygen species generation and precise targeting to tumors are crucial for photodynamic therapy (PDT). Here, a bromo-substituted diketopyrrolopyrrole derivative (2,5-bis(6-bromohexyl)-3,6-bis(5-bromothiophene-2-yl)-2,5-dihydropyrrolo[3,4-*c*]pyrrole-1,4-dione)-grafted hyaluronic acid is synthesized, which presents excellent targeting and PDT efficiency both in vitro and in vivo.

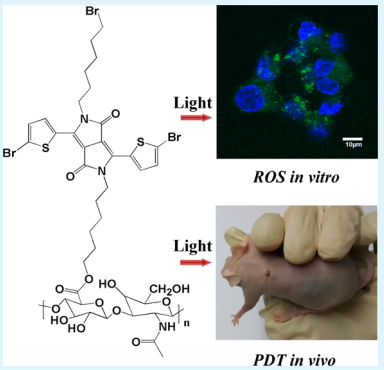

KEYWORDS: *photodynamic therapy, photosensitizers, diketopyrrolopyrrole, hyaluronic acid, bromo-substituted*

INTRODUCTION

Photodynamic therapy (PDT),[1−4] a promising strategy for cancer treatment, has drawn much attention due to the advantages of noninvasion, low systemic damage, and controllable therapy. To increase the photodynamic therapeutic efficacy, development of novel photosensitizers (PSs)[5,6] with high reactive oxygen species (ROS) generation and precisely targeting tumors are crucial. An efficient approach to improve the ROS generation is by incorporation of bromine atoms into the photosensitizer molecule to enhance the rate of intersystem crossing[7,8] (ISC) on the basis of the heavy atom effect. Recently, Shen and co-workers reported tribromo-substituted BODIPY exhibited higher singlet oxygen quantum yields due to the presence of bromo substitution. Besides low ROS generation of photosensitizers mentioned above, there are still other problems limiting its application in PDT, such as hydrophobicity, low photostability, no targeting to cancer cells, and so on.[9−11] Hence, it is strongly desirable to develop highly efficient photosensitizers with specific targeting, good biocompatibility, and photostability.[12,13]

Diketopyrrolopyrrole (DPP) derivatives[14−16] have been used widely in organic field effect transistors and fluorescent probes for anion and metal cation detection due to its excellent photostability, high molar absorption coefficient, and good fluorescence quantum yields. What is more, successful application of DPP derivatives in bioimaging[17] makes them possible candidates for biotherpy in the clinic. However, their low generation of singlet oxygen and nontargeting prevent their application in PDT.[18,19]

Herein, bromo-substituted DPP, 2,5-bis(6-bromohexyl)-3,6-bis(5-bromothiophene-2-yl)-2,5-dihydropyrrolo[3,4-*c*]pyrrole-1,4-dione (DTDPPBr2), was synthesized. Thienyl substituents were attached to the DPP moiety due to the more efficient π-conjugation capability compared to benzene, since it is known to greatly facilitate ISC,[20−23] and the bromine atoms were also introduced to enhance the ROS generation. Because of the excellent biocompatibility, hydrophilicity, and specific targeting to CD44 overexpressed tumor cells, hyaluronic acid (HA)[12,24] was selected to graft with DTDPPBr2, which can overcome both hydrophobicity and nonspecific targeting of PSs to tumor cells. Furthermore, the measurements in vitro and in vivo demonstrate that the obtained DTDPPBr2−HA presents low dark cytotoxicity, good biocompatibility, and excellent photodynamic therapeutic efficiency.

RESULTS AND DISCUSSION

The synthetic route of DTDPPBr2−HA is outlined in Scheme 1. The raw material was prepared according to the literature.[25,26] DTDPPBr2 and DTDPPBr2−HA were prepared in moderate to good isolated yields according to the established methods,[27] and the structures of the resulting compounds were characterized by ^{1}H NMR and ^{13}C NMR, respectively. Briefly, in the presence of KOH, the raw material first reacted with hexamethylene dibromide in DMF to give compound **1**. Then a

Received: February 4, 2016
Accepted: April 11, 2016
Published: April 11, 2016

DOI: 10.1021/acsami.6b01533
ACS Appl. Mater. Interfaces 2016, 8, 10737−10742

Scheme 1. Synthetic Route of DTDPPBr2−HA[a]

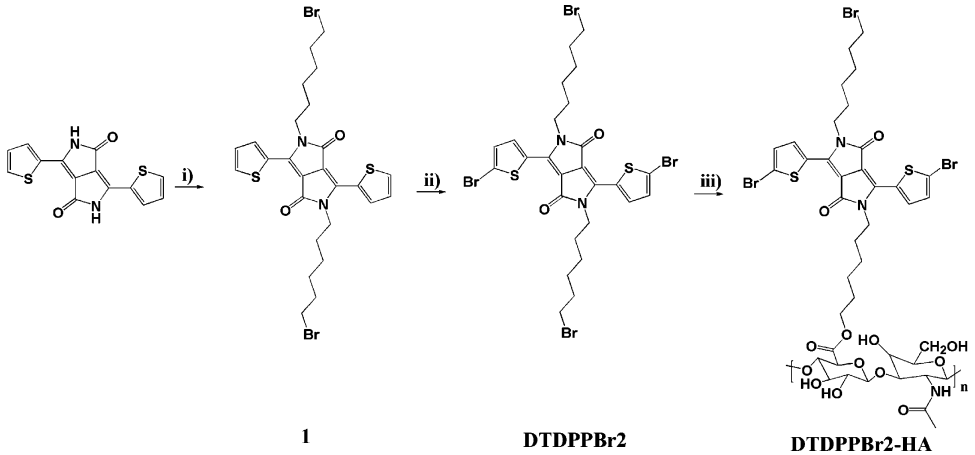

[a]Reagents and conditions: (i) KOH, hexamethylene dibromide, *N*,*N*-dimethylformamide, 65 °C, overnight, 52%; (ii) *N*-bromosuccinimide, chloroform, 25 °C, 6 h, 75%; (iii) sodium hyaluronate, tetrahydrofuran/acetone, 45 °C, 12 h, 42%.

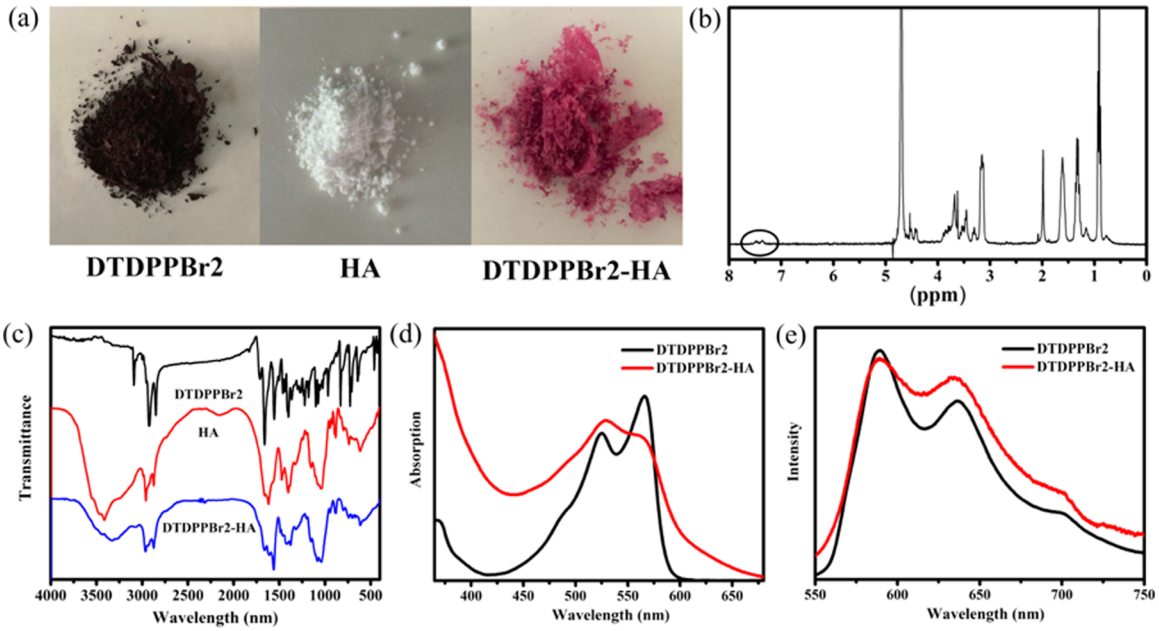

Figure 1. (a) Photographs of DTDPPBr2, HA, and DTDPPBr2−HA. (b) ^{1}H NMR spectrum of DTDPPBr2−HA in D_2O. (c) Infrared spectra of DTDPPBr2, HA, and DTDPPBr2−HA. (d) Normalized absorption spectra of DTDPPBr2 in DMF and DTDPPBr2−HA in H_2O. (e) Fluorescence emission spectra of DTDPPBr2 in DMF and DTDPPBr2−HA in H_2O.

mixture of compound **1** and *N*-bromosuccinimide (NBS) in chloroform was stirred at room temperature, producing DTDPPBr2. Finally, reaction of DTDPPBr2 and sodium hyaluronate resulted in the crude product DTDPPBr2−HA. After dialysis and freeze-drying, DTDPPBr2−HA was obtained. Different colors of the raw materials and desired product were observed, as shown in Figure 1a, and Figure S1 indicates that DTDPPBr2−HA presented a good water solubility even at a high concentration. Figure 1b shows the ^{1}H NMR spectra of DTDPPBr2−HA in D_2O. The expected signals of the thiophene moiety at around 7.3−7.5 ppm indicate the conjugation of DTDPPBr2 and HA, which cannot be found in pure HA.[28] In Figure 1c, the characteristic IR absorption peaks of DTDPPBr2−HA can be observed, and the overtone at 3431 cm^{-1} and the absorption peaks at 1154 and 1662 cm^{-1} suggest the existence of an ester group in DTDPPBr2−HA, which further proves the conjugation of DTDPPBr2 and HA. Figure 1d shows the absorption spectra of DTDPPBr2 and DTDPPBr2−HA. For DTDPPBr2, there are two obvious absorption peaks at 525 and 566 nm. It is well-known that HA has no apparent characteristic absorption in the UV−vis spectrum, but there are obvious absorption peaks for DTDPPBr2−HA at 528 and 560 nm. Figure 1e presents the fluorescence emission spectra of DTDPPBr2 and DTDPPBr2−HA. Two obvious fluorescence peaks are observed at about 589 and 636 nm, respectively, suggesting DTDPPBr2−HA has potential for bioimaging application.

To study the specific targeting to the CD44 receptor overexpressed cancer cells, HCT-116 cells were chosen to test the uptake of DTDPPBr2−HA, and A2780 cells were selected as a comparison.[29,30] As shown in Figure 2a, with the existence of DTDPPBr2−HA, HCT-116 cells exhibit obvious fluorescence (represented by a green color), while that of A2780 cells is rather weak. This phenomenon demonstrates that the

DOI: 10.1021/acsami.6b01533
ACS Appl. Mater. Interfaces 2016, 8, 10737−10742

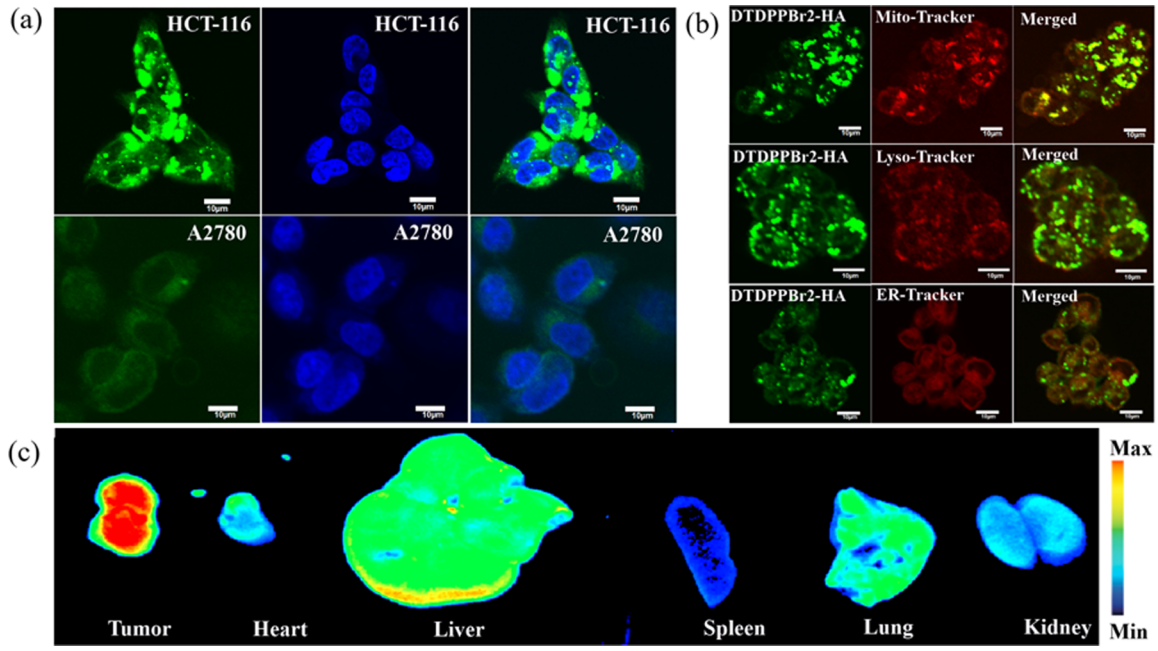

Figure 2. (a) Fluorescence images of DTDPPBr2−HA in HCT-116 and A2780 cells: left panel, fluorescence images; middle panel, DAPI channel; right panel, merged images. The green color represents the fluorescence of DTDPP−HA. (b) Subcellular localization of DTDPPBr2−HA in HCT-116 cells: left panel, DTDPPBr2−HA fluorescence images; middle panel, tracker channel; right panel, merged images. (c) Fluorescence images of DTDPPBr2−HA in HCT-116 tumor, heart, liver, spleen, lung, and kidney.

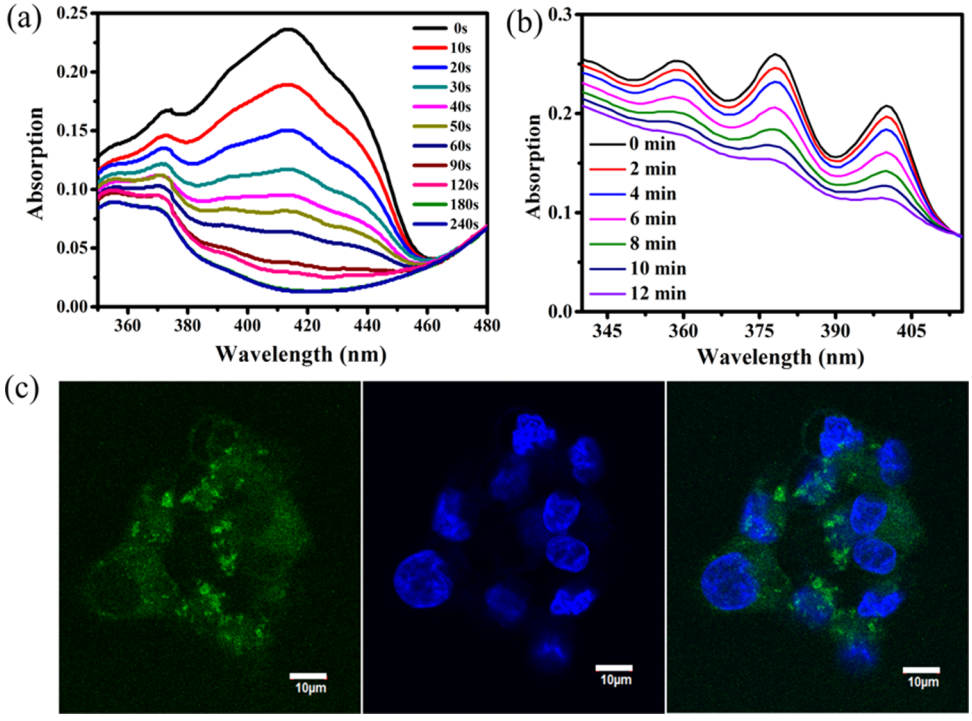

Figure 3. (a) Absorption spectra at 418 nm of DTDPPBr2 (10^{-5} mol/L) mixed with DPBF (10^{-5} mol/L) under illumination in DMF over time. (b) Absorption spectra at 379 nm of the mixture of DTDPPBr2−HA (2 mg/mL) and ABDA (10^{-5} mol/L) under illumination in DMSO/H_2O (v/v = 1/199) over time. (c) Confocal images of HCT-116 cells upon incubation with DTDPPBr2−HA and DCFH−DA upon light irradiation: left panel, fluorescence image; middle panel, DAPI channel, right panel, merged image.

DTDPPBr2−HA is selectively taken up and retained by HCT-116 cells through CD44 overexpression, and the difference between the fluorescence images indicates that the DTDPPBr2−HA has good specific targeting to CD44 receptor overexpressed cancer cells (e.g., HCT-116 cells). Subcellular localization of DTDPPBr2−HA in HCT-116 cells was also defined by using confocal microscopy and organelle-specific probes,[31] as shown in Figure 2b. The fluorescence (represented by the green color) of DTDPPBr2−HA and the fluorescence (represented by the red color) of mito-tracker or lyso-tracker on HCT-116 cells are largely overlapped, indicating

DOI: 10.1021/acsami.6b01533
ACS Appl. Mater. Interfaces 2016, 8, 10737−10742

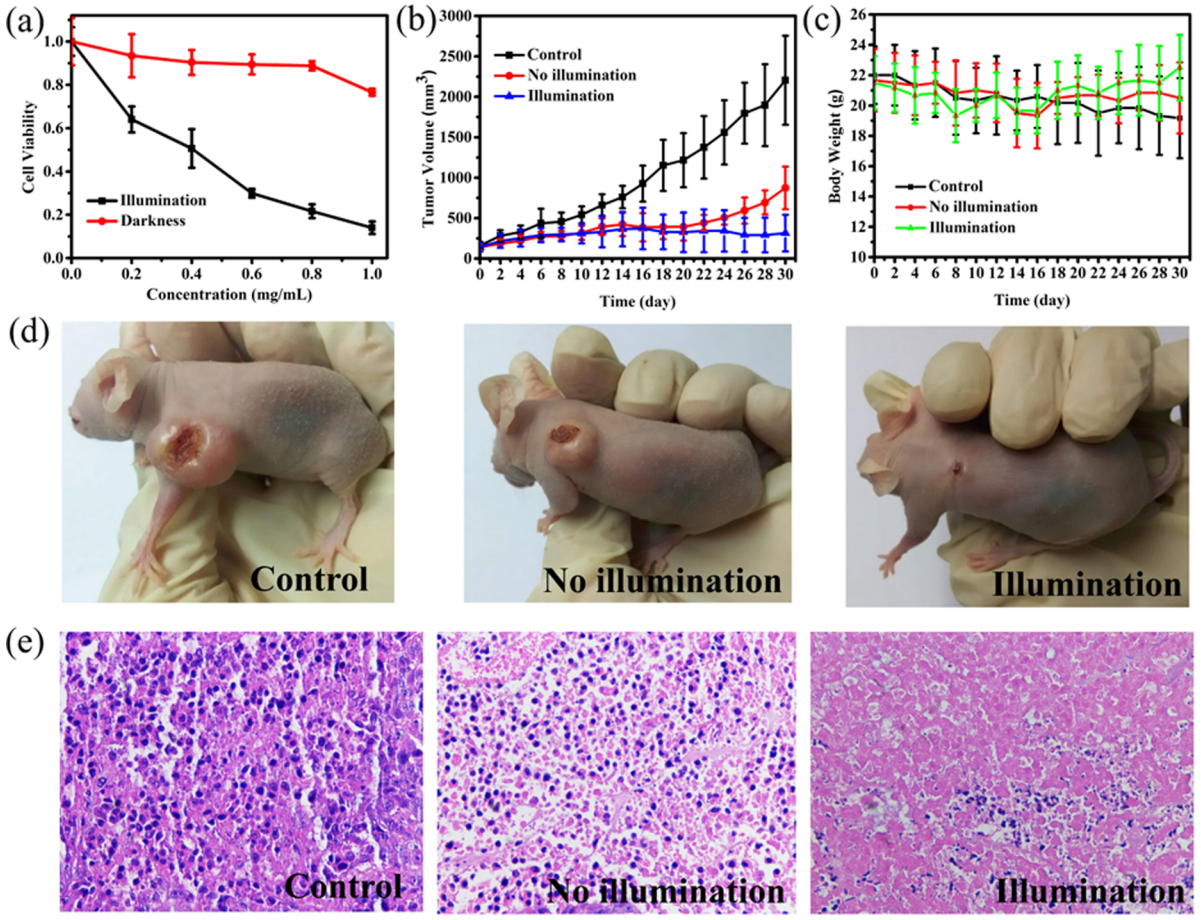

Figure 4. (a) Cell viability of HCT-116 treated with different concentrations of DTDPPBr2−HA with and without light illumination. (b) Relationship between tumor volume and time of each group after different treatments. (c) Change in the body weight of mice with time after different treatments. (d) Photographs of tumor-bearing mice treated after 30 days. (e) H&E-stained images of tumors from each group.

DTDPPBr2−HA is mainly located in the mitochondria or lysosome.

To further examine its tumor-targeting property, DTDPPBr2−HA (400 μg) was injected into HCT-116 tumor-bearing nude mice by tail veins.[7] After 24 h, the mice were sacrificed and the tumors and other organs were taken out for further fluorescence imaging study. As shown in Figure 2c, a strong fluorescence signal was observed in the tumor site due to the selective accumulation of DTDPPBr2−HA in the tumor. Only weak fluorescence can be observed in the liver, which is a detoxification organ, and no obvious fluorescence of DTDPPBr2−HA can be detected in the heart and spleen. Figure S5 shows the fluorescence images of tumors for no-overexpress CD44. They indicate that the DTDPPBr2−HA mainly aggregated into the heart, liver, and tumor, further suggesting DTDPPBr2−HA has an excellent targeting to HCT-116 tumors. These differences between fluorescence images of tumors and other organs further confirm that the DTDPPBr2−HA has an excellent targeting property toward HCT-116 tumor in vivo, which could effectively avoid accidental injury of other normal organs.

Cytotoxic reactive oxygen species, especially singlet oxygen ($^1O_2$), proved to result in irreversible cell damage and cause cell death and tumor destruction in PDT. The $^1O_2$ generation ability of DTDPPBr2 is examined by using 3-diphenylisobenzofuran (DPBF)[32] as an indicator with the absorption peak at 418 nm and the absorption intensity weakening upon reaction with $^1O_2$. As shown in Figure 3a, the absorption intensity of the DTDPPBr2 and DPBF mixture at 418 nm decreases significantly compared with that of compound **1** (Figure S4) after irradiation and almost disappears in 90 s, indicating the excellent $^1O_2$ generation ability of DTDPPBr2 (the yield of singlet oxygen is about 16.2%). Meanwhile, the $^1O_2$ generation efficiency of DTDPPBr2−HA is also measured by using 9,10-anthracenediylbis(methylene)dimalonic acid (ABDA)[33] as an indicator. As shown in Figure 3b, under illumination, the absorption density of ABDA at 378 nm decreases gradually with prolonged time, indicating DTDPPBr2−HA produces $^1O_2$ with high efficiency in a water solution. 2′,7′-Dichlorofluorescein diacetate (DCFH−DA) is an ROS probe[34] in HCT-116 cells. While DCFH−DA reacts with ROS, fluorescent 2′,7′-dichlorofluorescein (DCF) is produced. Figure 3c shows the fluorescence images of DTDPPBr2−HA with DCFH−DA as an indicator in HCT-116 cells upon light irradiation. After 2min of irradiation, strong fluorescence was observed, which can be ascribed to the reaction of DCFH−DA with ROS in HCT-116 cells, confirming the high $^1O_2$ generation ability of DTDPPBr2−HA in cells.

Low dark cytotoxicity and high light cytotoxicity are the key properties of the PSs for their application in PDT.[35] As shown in Figure 4a, DTDPPBr2−HA presents a low cytotoxic effect on HCT-116 cells in the dark even at a high concentration. On the contrary, the DTDPPBr2−HA exhibits a concentration-dependent PDT effect under light irradiation (510 nm, 40

DOI: 10.1021/acsami.6b01533
ACS Appl. Mater. Interfaces 2016, 8, 10737−10742

mW/cm^2, 7 min). The half-maximal inhibitory concentration (IC_{50}) of DTDPPBr2−HA is 0.4 mg/mL, demonstrating high $^1O_2$ generation in DTDPPBr2−HA-incubated cells and an excellent PDT effect under 510 nm light illumination.

To further evaluate the PDT therapeutic efficacy in vivo, the DTDPPBr2−HA (400 μg) was tail vein injected into HCT-116 tumor-bearing mice (six mice per group), and the changes in the tumor volumes and body weight were recorded. As shown in Figure 4b,d, the tumor volumes of the control group increased rapidly. However, the tumor volumes of the injected group increased steadily without additional light irradiation due to the room light everywhere. In contrast, DTDPPBr2−HA under light irradiation can remarkably inhibit the tumor growth. Moreover, the volumes of the tumors regressed after 16 days and almost disappeared after 30 days of treatment, which implies that DTDPPBr2−HA has excellent PDT therapeutic efficacy. Meanwhile, the relative body weight of mice in the control group decreased gradually (Figure 4c). No obvious weight loss was observed for the mice treated with DTDPPBr2−HA under light irradiation, suggesting negligible systemic toxicity of DTDPPBr2−HA to mice. Figure 4d shows the photographs of three mice from the three groups after treatment for 30 days, which more intuitive proves the PDT effect of DTDPPBr2−HA. The hematoxylin and eosin (H&E)-stained images of the tumor histologic section of each group are shown in Figure 4e. Compared to the control and without illumination groups, obvious apoptosis can be observed for the tumor treated by DTDPPBr2−HA under illumination, and the nucleus became smaller and the color of staining became shallower. H&E-stained images of the major organs from the three groups were also analyzed, and there is no significant difference between these two groups, which means low tissue toxicity of DTDPPBr2−HA (Figure S6). These results further demonstrate that the DTDPPBr2−HA can serve as a potential targeting photosensitizer for PDT to kill tumor cells clinically.

CONCLUSION

In summary, a novel PDT photosensitizer, a bromo-substituted DPP derivative (DTDPPBr2−HA), has been developed, which is modified by HA to increase its water solubility. The DTDPPBr2−HA with high singlet oxygen generation exhibits specific targeting to the CD44 receptor overexpressed cancer cells and effectively suppresses tumor growth in both in vitro and in vivo experiments. Therefore, the DTDPPBr2−HA with dark toxicity and high phototoxicity would be a potential and promising theranostic agent for PDT treatment in the clinic.

ASSOCIATED CONTENT

Supporting Information

The Supporting Information is available free of charge on the ACS Publications website at DOI: 10.1021/acsami.6b01533.

Experimental details, photographs of DTDPPBr2 and DTDPPBr2−HA in water (Figure S1), fluorescence emission spectrum of compound **1** (Figure S2), MALDI-TOF mass spectrum of DTDPPBr2−HA (Figure S3), singlet oxygen generation of compound **1** (Figure S4), fluorescence images of DTDPPBr2−HA in Hela tumor, heart, liver, spleen, lung, and kidney (Figure S5), and H&E-stained images (Figure S6) (PDF)

AUTHOR INFORMATION

Corresponding Authors

*E-mail: zhangqi@njtech.edu.cn.
*E-mail: iamwhuang@njtech.edu.cn.
*E-mail: iamxcdong@njtech.edu.cn.

Notes

The authors declare no competing financial interest.

ACKNOWLEDGMENTS

This work was supported by the 973 program (Grant 2014CB660808), the National Natural Science Foundation of China (Grants 61525402 and 21275076), the Key University Science Research Project of Jiangsu Province (Grant 15KJA430006), Jiangsu Provincial Funds for Distinguished Young Scholars (Grant BK20130046), the Program for New Century Excellent Talents in University (Grant NCET-13-0853), the QingLan Project, and the Priority Academic Program Development of Jiangsu Higher Education Institutions (PAPD).

REFERENCES

(1) Kamkaew, A.; Lim, S. H.; Lee, H. B.; Kiew, L. V.; Chung, L. Y.; Burgess, K. BODIPY Dyes in Photodynamic Therapy. *Chem. Soc. Rev.* **2013**, *42*, 77−88.

(2) Chang, C. C.; Hsieh, M. C.; Lin, J. C.; Chang, T. C. Selective Photodynamic Therapy Based on Aggregation-Induced Emission Enhancement of Fluorescent Organic Nanoparticles. *Biomaterials* **2012**, *33*, 897−906.

(3) Schmitt, J.; Heitz, V.; Sour, A.; Bolze, F.; Ftouni, H.; Nicoud, J. F.; Flamigni, L.; Ventura, B. Diketopyrrolopyrrole-Porphyrin Conjugates with High Two-Photon Absorption and Singlet Oxygen Generation for Two-photon Photodynamic Therapy. *Angew. Chem., Int. Ed.* **2015**, *54*, 169−173.

(4) Secret, E.; Maynadier, M.; Gallud, A.; Chaix, A.; Bouffard, E.; Gary-Bobo, M.; Marcotte, N.; Mongin, O.; El Cheikh, K.; Hugues, V.; Auffan, M.; Frochot, C.; Morere, A.; Maillard, P.; Blanchard-Desce, M.; Sailor, M. J.; Garcia, M.; Durand, J. O.; Cunin, F. Two-Photon Excitation of Porphyrin-Functionalized Porous Silicon Nanoparticles for Photodynamic Therapy. *Adv. Mater.* **2014**, *26*, 7643−7648.

(5) Tian, J.; Zhou, J.; Shen, Z.; Ding, L.; Yu, J.-S.; Ju, H. A pH-Activatable and Aniline-Substituted Photosensitizer for Near-infrared Cancer Theranostics. *Chem. Sci.* **2015**, *6*, 5969−5977.

(6) Haedicke, K.; Grafe, S.; Lehmann, F.; Hilger, I. Multiplexed in Vivo Fluorescence Optical Imaging of the Therapeutic Efficacy of Photodynamic Therapy. *Biomaterials* **2013**, *34*, 10075−10083.

(7) Zhang, C.; Li, C.; Liu, Y.; Zhang, J.; Bao, C.; Liang, S.; Wang, Q.; Yang, Y.; Fu, H.; Wang, K.; Cui, D. Gold Nanoclusters-Based Nanoprobes for Simultaneous Fluorescence Imaging and Targeted Photodynamic Therapy with Superior Penetration and Retention Behavior in Tumors. *Adv. Funct. Mater.* **2015**, *25*, 1314−1325.

(8) Zhao, J.; Wu, W.; Sun, J.; Guo, S. Triplet Photosensitizers: from Molecular Design to Applications. *Chem. Soc. Rev.* **2013**, *42*, 5323−5351.

(9) Shi, J.; Yu, X.; Wang, L.; Liu, Y.; Gao, J.; Zhang, J.; Ma, R.; Liu, R.; Zhang, Z. PEGylated Fullerene/Iron Oxide Nanocomposites for Photodynamic Therapy, Targeted Drug Delivery and MR Imaging. *Biomaterials* **2013**, *34*, 9666−9677.

(10) Li, Z.; Wang, C.; Cheng, L.; Gong, H.; Yin, S.; Gong, Q.; Li, Y.; Liu, Z. PEG-Functionalized Iron Oxide Nanoclusters Loaded with Chlorin e6 for Targeted, NIR Light Induced, Photodynamic Therapy. *Biomaterials* **2013**, *34*, 9160−9170.

(11) Eshghi, H.; Sazgarnia, A.; Rahimizadeh, M.; Attaran, N.; Bakavoli, M.; Soudmand, S. Protoporphyrin IX-Gold Nanoparticle Conjugates as an Efficient Photosensitizer in Cervical Cancer Therapy. *Photodiagn. Photodyn. Ther.* **2013**, *10*, 304−312.

DOI: 10.1021/acsami.6b01533
ACS Appl. Mater. Interfaces 2016, 8, 10737−10742

(12) Yoon, H. Y.; Koo, H.; Choi, K. Y.; Lee, S. J.; Kim, K.; Kwon, I. C.; Leary, J. F.; Park, K.; Yuk, S. H.; Park, J. H.; Choi, K. Tumor-Targeting Hyaluronic Acid Nanoparticles for Photodynamic Imaging and Therapy. *Biomaterials* **2012**, *33*, 3980−3989.
(13) Terreno, E.; Uggeri, F.; Aime, S. Image Guided Therapy: the Advent of Theranostic Agents. *J. Controlled Release* **2012**, *161*, 328−337.
(14) Yi, Z.; Wang, S.; Liu, Y. Design of High-Mobility Diketopyrrolopyrrole-Based pi-Conjugated Copolymers for Organic Thin-Film Transistors. *Adv. Mater.* **2015**, *27*, 3589−3606.
(15) Wang, J.-L.; Wu, Z.; Miao, J.-S.; Liu, K.-K.; Chang, Z.-F.; Zhang, R.-B.; Wu, H.-B.; Cao, Y. Solution-Processed Diketopyrrolopyrrole-Containing Small-Molecule Organic Solar Cells with 7.0% Efficiency: In-Depth Investigation on the Effects of Structure Modification and Solvent Vapor Annealing. *Chem. Mater.* **2015**, *27*, 4338−4348.
(16) Zhang, G.; Song, L.; Bi, S.; Wu, Y.; Yu, J.; Wang, L. Mild Synthesis and Photophysical Properties of Symmetrically Substituted Diketopyrrolopyrrole Derivatives. *Dyes Pigm.* **2014**, *102*, 100−106.
(17) Kaur, M.; Choi, D. H. Diketopyrrolopyrrole: Brilliant Red Pigment Dye-Based Fluorescent Probes and their Applications. *Chem. Soc. Rev.* **2015**, *44*, 58−77.
(18) Burckstummer, H.; Weissenstein, A.; Bialas, D.; Wurthner, F. Synthesis and Characterization of Optical and Redox Properties of Bithiophene-Functionalized Diketopyrrolopyrrole Chromophores. *J. Org. Chem.* **2011**, *76*, 2426−2432.
(19) Guo, E. Q.; Ren, P. H.; Zhang, Y. L.; Zhang, H. C.; Yang, W. J. Diphenylamine End-Capped 1,4-diketo-3,6-diphenylpyrrolo[3,4-c]-pyrrole (DPP) Derivatives with Large Two-Photon Absorption Cross-Sections and Strong Two-Photon Excitation Red Fluorescence. *Chem. Commun.* **2009**, 5859−5861.
(20) Varanasi, P. R.; Jen, A. K. Y.; Chandrasekhar, J.; Namboothiri, I. N. N.; Rathna, A. The Important Role of Heteroaromatics in the Design of Efficient Second-Order Nonlinear Optical Molecules: Theoretical Investigation on Push-Pull Heteroaromatic Stilbenes. *J. Am. Chem. Soc.* **1996**, *118*, 12443−12448.
(21) Yang, Y.; Guo, Q.; Chen, H.; Zhou, Z.; Guo, Z.; Shen, Z. Thienopyrrole-Expanded BODIPY as a Potential NIR Photosensitizer for Photodynamic Therapy. *Chem. Commun.* **2013**, *49*, 3940−3942.
(22) Kim, S.; Ohulchanskyy, T. Y.; Pudavar, H. E.; Pandey, R. K.; Prasad, P. N. Organically Modified Silica Nanoparticles Co-Encapsulating Photosensitizing Drug and Aggregation-Enhanced Two-Photon Absorbing Fluorescent Dye Aggregates for Two-Photon Photodynamic Therapy. *J. Am. Chem. Soc.* **2007**, *129*, 2669−2675.
(23) Kim, S.; Ohulchanskyy, T. Y.; Baev, A.; Prasad, P. N. Synthesis and Nanoparticle Encapsulation of 3,5-difuranylvinyl-boradiaza-s-indacenes for Near-Infrared Fluorescence Imaging. *J. Mater. Chem.* **2009**, *19*, 3181−3188.
(24) Tran, T. H.; Choi, J. Y.; Ramasamy, T.; Truong, D. H.; Nguyen, C. N.; Choi, H. G.; Yong, C. S.; Kim, J. O. Hyaluronic Acid-Coated Solid Lipid Nanoparticles for Targeted Delivery of Vorinostat to CD44 Overexpressing Cancer Cells. *Carbohydr. Polym.* **2014**, *114*, 407−415.
(25) Ghazvini Zadeh, E. H.; Bondar, M. V.; Mikhailov, I. A.; Belfield, K. D. Linear Photophysics, Stimulated Emission, and Ultrafast Spectroscopy of New Two-Photon Absorbing Diketopyrrolopyrrole Derivatives. *J. Phys. Chem. C* **2015**, *119*, 8864−8875.
(26) Zhou, R.; Li, Q.-D.; Li, X.-C.; Lu, S.-M.; Wang, L.-P.; Zhang, C.-H.; Huang, J.; Chen, P.; Li, F.; Zhu, X.-H.; Choy, W. C. H.; Peng, J.; Cao, Y.; Gong, X. A Solution-Processable Diketopyrrolopyrrole Dye Molecule with (Fluoronaphthyl)thienyl Endgroups for Organic Solar Cells. *Dyes Pigm.* **2014**, *101*, 51−57.
(27) Kanimozhi, C.; Yaacobi-Gross, N.; Chou, K. W.; Amassian, A.; Anthopoulos, T. D.; Patil, S. Diketopyrrolopyrrole-Diketopyrrolopyrrole-Based Conjugated Copolymer for High-Mobility Organic Field-Effect Transistors. *J. Am. Chem. Soc.* **2012**, *134*, 16532−16535.
(28) Vasi, A. M.; Popa, M. I.; Butnaru, M.; Dodi, G.; Verestiuc, L. Chemical Functionalization of Hyaluronic Acid for Drug Delivery Applications. *Mater. Sci. Eng., C* **2014**, *38*, 177−185.
(29) Yamada, Y.; Hashida, M.; Harashima, H. Hyaluronic Acid Controls the Uptake Pathway and Intracellular Trafficking of an Octaarginine-Modified Gene Vector in CD44 Positive- and CD44 Negative-Cells. *Biomaterials* **2015**, *52*, 189−198.
(30) Lee, G. Y.; Kim, J. H.; Choi, K. Y.; Yoon, H. Y.; Kim, K.; Kwon, I. C.; Choi, K.; Lee, B. H.; Park, J. H.; Kim, I. S. Hyaluronic Acid Nanoparticles for Active Targeting Atherosclerosis. *Biomaterials* **2015**, *53*, 341−348.
(31) Xu, H.; He, J.; Zhang, Y.; Fan, L.; Zhao, Y.; Xu, T.; Nie, Z.; Li, X.; Huang, Z.; Lu, B.; Xu, P. Synthesis and in Vitro Evaluation of a Hyaluronic Acid-Quantum Dots-Melphalan Conjugate. *Carbohydr. Polym.* **2015**, *121*, 132−139.
(32) Zhang, L.; Lei, J.; Ma, F.; Ling, P.; Liu, J.; Ju, H. A Porphyrin Photosensitized Metal-Organic Framework for Cancer Cell Apoptosis and Caspase Responsive Theranostics. *Chem. Commun.* **2015**, *51*, 10831−10834.
(33) Yuan, Y.; Zhang, C. J.; Liu, B. A Platinum Prodrug Conjugated with a Photosensitizer with Aggregation-Induced Emission (AIE) Characteristics for Drug Activation Monitoring and Combinatorial Photodynamic-Chemotherapy against Cisplatin Resistant Cancer Cells. *Chem. Commun.* **2015**, *51*, 8626−8629.
(34) Wang, L.; Shi, J.; Liu, R.; Liu, Y.; Zhang, J.; Yu, X.; Gao, J.; Zhang, C.; Zhang, Z. Photodynamic Effect of Functionalized Single-Walled Carbon Nanotubes: a Potential Sensitizer for Photodynamic Therapy. *Nanoscale* **2014**, *6*, 4642−4651.
(35) Xia, L.; Kong, X.; Liu, X.; Tu, L.; Zhang, Y.; Chang, Y.; Liu, K.; Shen, D.; Zhao, H.; Zhang, H. An Upconversion Nanoparticle–Zinc Phthalocyanine based Nanophotosensitizer for Photodynamic Therapy. *Biomaterials* **2014**, *35*, 4146−4156.

DOI: 10.1021/acsami.6b01533
ACS Appl. Mater. Interfaces 2016, 8, 10737−10742